Journal of Medicinal Chemistry

pubs.acs.org/jmc

Article

Design, Synthesis, and Biological Evaluation of New Peripheral $5HT_{2A}$ Antagonists for Nonalcoholic Fatty Liver Disease

Minhee Kim,[‡] Inseon Hwang,[‡] Haushabhau S. Pagire, Suvarna H. Pagire, Wonsuk Choi, Won Gun Choi, Jihyeon Yoon, Won Mi Lee, Jin Sook Song, Eun Kyung Yoo, Seung Mi Lee, Mi-jin Kim, Myung Ae Bae, Dooseop Kim, Heejong Lee, Eun-Young Lee, Jae-Han Jeon, In-Kyu Lee, Hail Kim,* and Jin Hee Ahn*

Cite This: https://dx.doi.org/10.1021/acs.jmedchem.0c00002

Read Online

ACCESS | Metrics & More | Article Recommendations | Supporting Information

ABSTRACT: Nonalcoholic fatty liver disease (NAFLD) is increasingly prevalent worldwide, causing serious liver complications, including non-alcoholic steatohepatitis. Recent findings suggest that peripheral serotonin (5-hydroxytryptamine, 5HT) regulates energy homeostasis, including hepatic lipid metabolism. More specifically, liver-specific $5HT_{2A}$ knockout mice exhibit alleviated hepatic lipid accumulation and hepatic steatosis. Here, structural modifications of pimavanserin (CNS drug), a $5HT_{2A}$ antagonist approved for Parkinson's disease, led us to synthesize new peripherally acting $5HT_{2A}$ antagonists. Among the synthesized compounds, compound **14a** showed good in vitro activity, good liver microsomal stability, 5HT subtype selectivity, and no significant inhibition of CYP and hERG. The in vitro and in vivo blood–brain barrier permeability study proved that **14a** acts peripherally. Compound **14a** decreased the liver weight and hepatic lipid accumulation in high-fat-diet-induced obesity mice. Our study suggests new therapeutic possibilities for peripheral $5HT_{2A}$ antagonists in NAFLD.

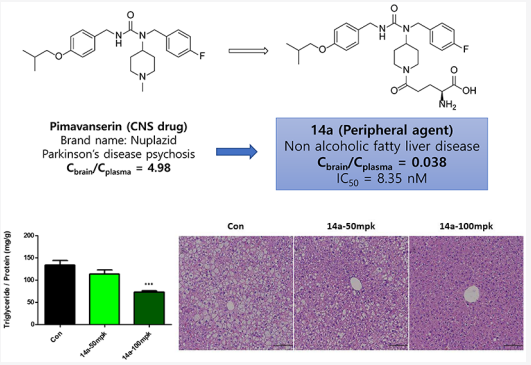

INTRODUCTION

Nonalcoholic fatty liver disease (NAFLD), which involves excessive lipid accumulation in the liver, has become a serious disease worldwide.[1,2] It is closely associated with obesity and chronic liver disease and is considered a leading cause of progressive liver affections such as nonalcoholic steatohepatitis (NASH), cirrhosis, and hepatocellular carcinoma.[3,4] Serotonin (5-hydroxytryptamine, 5HT) is a monoamine mostly found in the gastrointestinal tract, platelets, and the pineal gland, and in smaller amounts in the brain.[5−8] In the central nervous system (CNS), 5HT acts as a neurotransmitter that modulates mood, behavior, sleep cycles, and appetite.[9−14] Central and peripheral serotonin systems are regarded as separate systems because 5HT cannot cross the blood–brain barrier (BBB).[9,15,16]

The physiology of peripheral 5HT has been studied since the 1960s, and recent findings suggest that peripheral 5HT can regulate energy homeostasis.[16−18] Slc6a4 (serotonin transporter, SERT) knockout mice manifested an obese phenotype with a metabolic syndrome,[17] and TPH1/TPH2 (tryptophan hydroxylase 1 and 2) double knockout (DKO) mice displayed reduced body weight.[18] In addition, inhibition of 5HT synthesis elicited decreased lipogenesis in the epididymal white adipose tissue (WAT), induction of browning in the inguinal WAT, and activation of adaptive thermogenesis in brown adipose tissue (BAT).[16,19−21] Other studies indicate that peripheral 5HT can also regulate hepatic lipid metabolism.[21−24] Among the subtypes of 5HT receptors, liver-specific $5HT_{2A}$ knockout mice showed a reduction in liver size, weight, and lipid accumulation, as indicated by histological data, NAS (NAFLD activity score), and hepatic triglyceride (TG) concentrations, without affecting the systemic energy homeostasis.[23]

These biological results prompted us to identify new peripheral $5HT_{2A}$ antagonists. Many $5HT_{2A}$ antagonists are currently being used for CNS disorders, including schizophrenia. We envisioned new peripheral $5HT_{2A}$ antagonists by introducing non-BBB-permeable moieties on CNS drugs. We chose pimavanserin (Nuplazid), 1-(4-fluorobenzyl)-3-(4-isobutoxybenzyl)-1-)1-methylpiperidin-4-yl)urea (**1**), a $5HT_{2A}$ antagonist approved in 2016 in the United States for Parkinson's disease,[25] for structural modification (Figure 1 and Table 1).

Diverse derivatives are designed and synthesized with the aim of obtaining peripherally acting compounds. In the present

Received: January 4, 2020

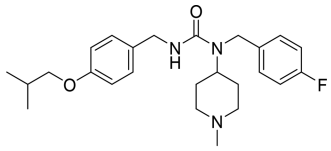

1

Figure 1. Chemical structure of compound **1** (pimavanserin).

Table 1. Brain/Plasma Ratio in Male ICR Mice (10 mg/kg, ip, Mean ± SD, n = 3) for Compound 1

	concentration (ng/mL or ng/g)		
time (h)	plasma	brain tissue	C_{brain}/C_{plasma}
0.5	612.0 ± 49.0	3014 ± 590.6	4.98 ± 1.25

study, we report the synthesis and biological evaluation of new peripherally acting $5HT_{2A}$ antagonists.

RESULTS AND DISCUSSION

A new series of $5HT_{2A}$ antagonists were synthesized according to synthesis Schemes 1–6. The commercially available 4-hydroxybenzylamine (**2**) was treated with di-*tert*-butyl dicarbonate resulting in compound **3**. Compound **3** reacted with 1-bromo-2-methylpropane under alkaline conditions to afford compound **4**. Compound **5** was synthesized by the acidic deprotection of compound **4**. Compound **5** treated with 1,1′-carbonyldiimidazole (CDI) afforded compound **6**. Compound **10** was obtained under alkaline conditions through a coupling reaction between compound **6** and compound **9**, which was synthesized through the reductive amination of commercially available 4-fluorobenzaldehyde (**7**) and 1-Boc-4-piperidineamine (**8**) to give compound **10**. Compound **10** underwent acidic deprotection leading to compound **11**, *N*-desmethylpimavanserin (Scheme 1). Compounds **12a–c** were synthesized through the reaction of compound **11** and acetyl chloride, methanesulfonyl chloride, and isopropyl thiocyanate, respectively, in the presence of a base. The condensation of compound **11** and succinic anhydride afforded compound **13** (Scheme 2). The amide coupling reaction of compound **11** and 1-benzyl *N*-carbobenzoxy-L-glutamate, 1-benzyl *N*-benzyloxycarbonyl-L-aspartate, and 5-benzyl *N*-benzyloxycarbonyl-L-glutamate afforded coupled products followed by hydrogenation resulting in compounds **14a-c**, respectively. Compound **14a** was treated with di-*tert*-butyl dicarbonate under alkaline conditions to produce compound **15** (Scheme 3). Commercially available L-tyrosine (**16**) underwent esterification to give compound **17**. Compound **17** was treated with di-*tert*-butyl dicarbonate to afford compound **18**. The condensation of compound **18** and trifluoromethanesulfonic anhydride yielded compound **19**. Compound **19** was converted into carboxylic acid to give compound **20**. Compound **11** was coupled with compound **20** affording compound **21** and after hydrolysis and acidic deprotection compound **22** was obtained (Scheme 4).

The reaction between 4-hydroxybenzylamine (**2**) and phthalic anhydride resulted in compound **23**. Compound **23** reacted with epichlorohydrin in the presence of a base to afford

Scheme 1. Synthesis of *N*-Desmethylpimavanserin (Compound 11)[a]

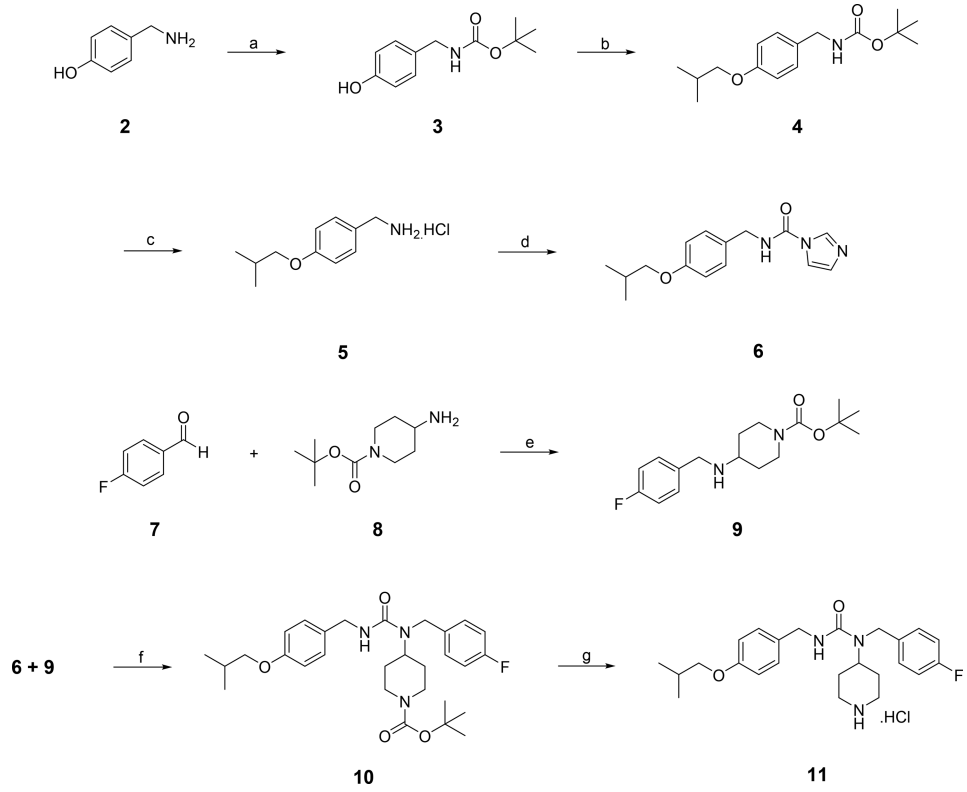

2 3 4 5 6 7 8 9 10 11

[a]Reagents and conditions: (a) di-*tert*-butyl dicarbonate, $NaHCO_3$, MeOH, H_2O, rt, 95%; (b) 1-bromo-2-methylpropane, K_2CO_3, DMF, 80 °C, 32%; (c) 4 M HCl in 1,4-dioxane, EtOAc, rt, 92%; (d) 1,1′-carbonyldiimidazole, DMF, rt, 68%; (e) $NaBH_4$, MeOH, rt, 65%; (f) K_2CO_3, DMF, rt, 74%; and (g) 4 M HCl in 1,4-dioxane, EtOAc, rt, 88%.

https://dx.doi.org/10.1021/acs.jmedchem.0c00002
J. Med. Chem. XXXX, XXX, XXX–XXX

Scheme 2. Synthesis Acetyl, Methanesulfonyl, Isopropylthiocyanate, and Succinyl Derivatives of Pimavanserin (Compounds 12a-c and 13)[a]

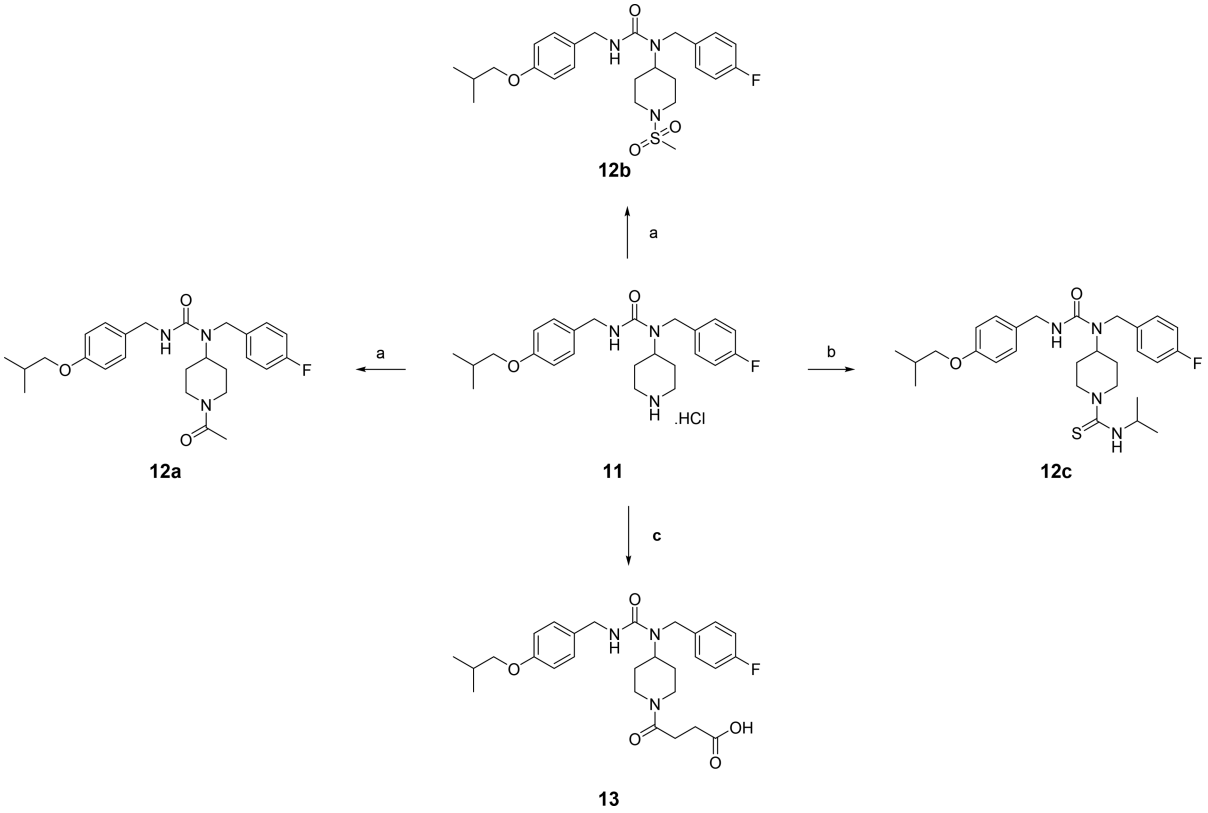

[a]Reagents and conditions: (a) acetyl chloride or methanesulfonyl chloride, DIPEA, DCM, 0 °C to rt, 61−79%; (b) Isopropyl isothiocyanate, DIPEA, THF, 40 °C, 97%; and (c) succinic anhydride, THF, reflux, 61%.

Scheme 3. Synthesis of Amino Acid Derivatives of Pimavanserin (Compounds 14a−c and 15)[a]

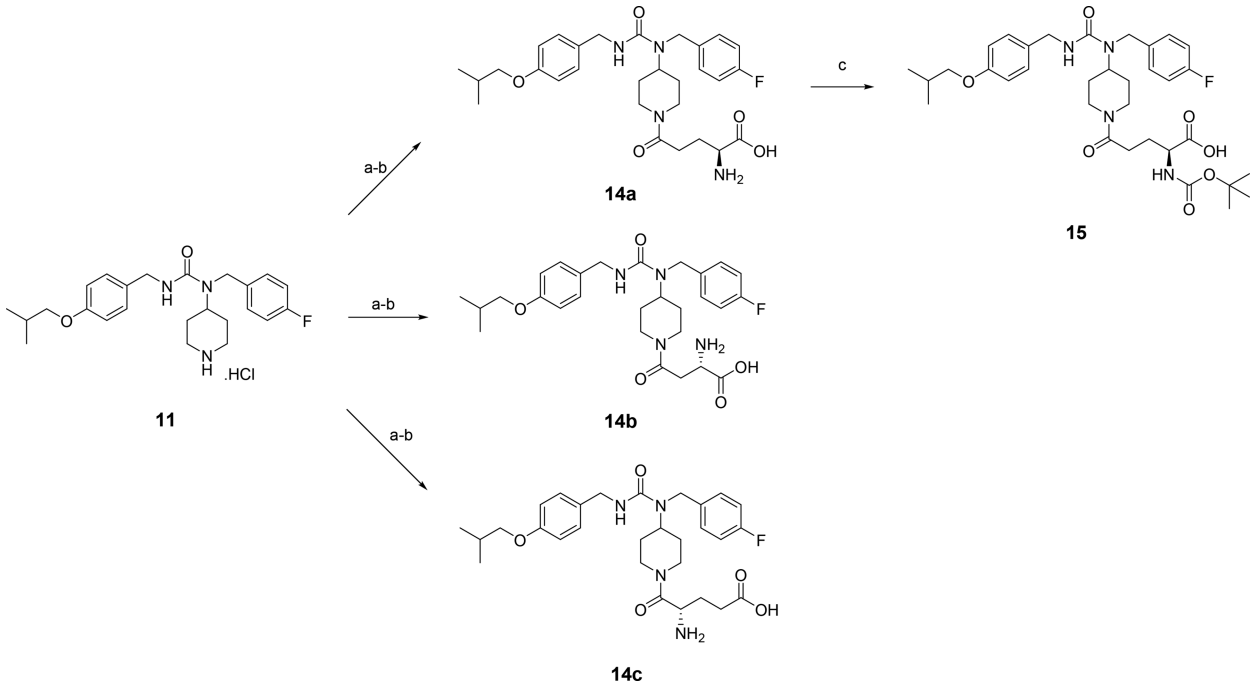

[a]Reagents and conditions: (a) 1-benzyl *N*-carbobenzoxy-L-glutamate or 1-benzyl *N*-benzyloxycarbonyl-L-aspartate or 5-benzyl *N*-benzyloxycarbonyl-L-gluatamte, EDCI, HOBt, DIPEA, DMF, rt, 44−73%; (b) H_2, Pd/C, MeOH, rt, 63−75%; and (c) di-*tert*-butyl dicarbonate, NaOH, 1,4-dioxane, H_2O, rt, 84%.

https://dx.doi.org/10.1021/acs.jmedchem.0c00002
J. Med. Chem. XXXX, XXX, XXX−XXX

Scheme 4. Synthesis of the Tyrosine Derivative of Pimavanserin (Compound 22)[a]

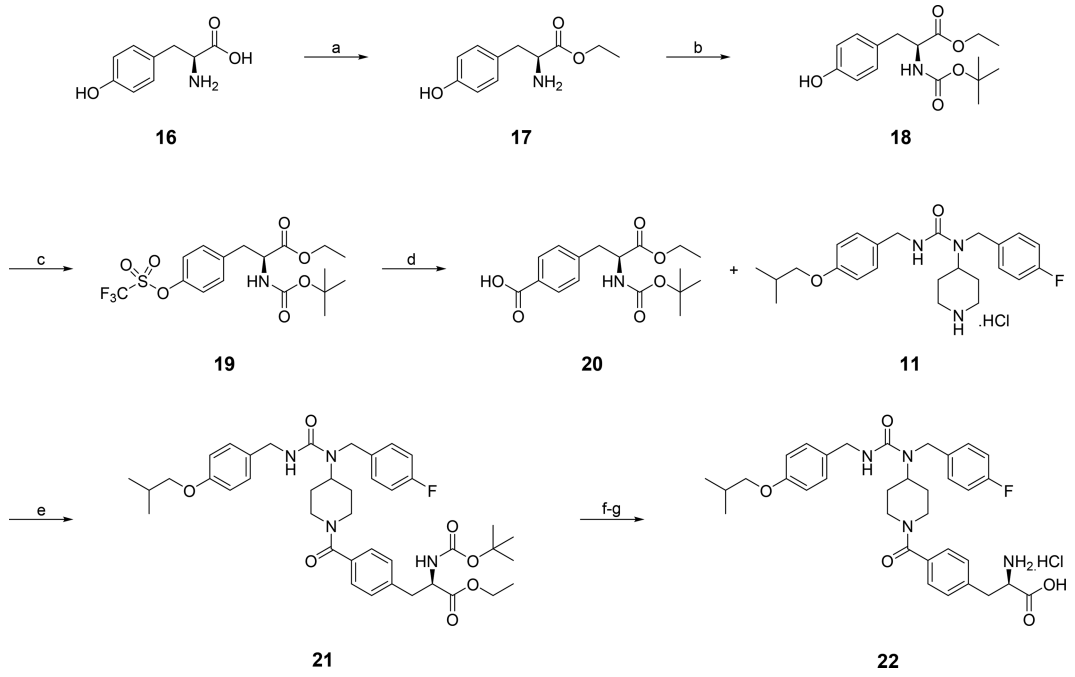

[a]Reagents and conditions: (a) $SOCl_2$, EtOH, reflux; (b) Boc_2O, TEA, MeOH, DCM, rt, 80%; (c) $(CF_3SO_2)_2O$, pyridine, DCM, rt, 95%; (d) $Pd(OAc)_2$, dppf, $V(CO)_6$, DMAP, DIPEA, H_2O, 1,4-dioxane, microwave, 110 °C, 78%; (e) EDCI, HOBt, DIPEA, DMF, rt, 74%; (f) NaOH, THF, H_2O, rt, 86%; and (g) 4 M HCl in 1,4-dioxane, EtOAc, rt, 83%.

Scheme 5. Synthesis of Amino Alcohol Derivatives of Pimavanserin (Compounds 30 and 31)[a]

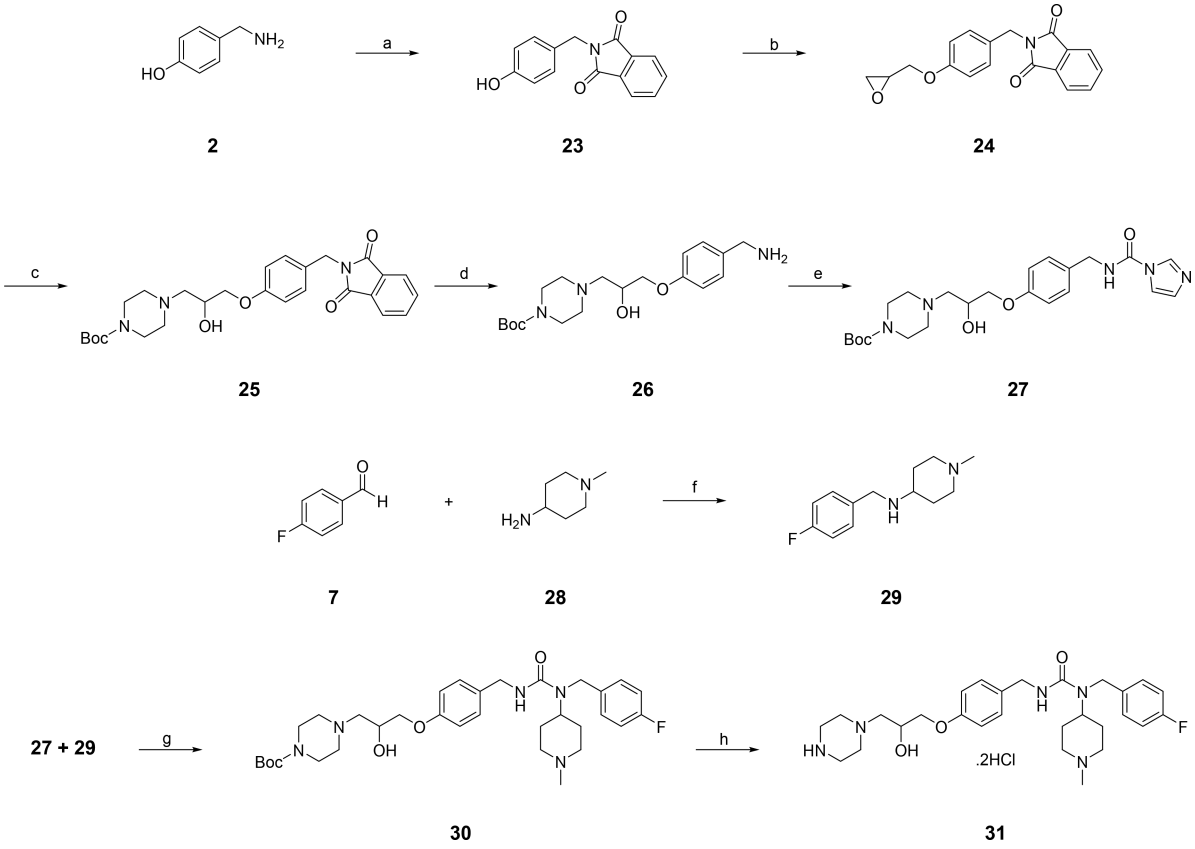

[a]Reagents and conditions: (a) phthalic anhydride, DMF, 140 °C, 32%; (b) epichlorohydrin, K_2CO_3, ACN, reflux, 50%; (c) 1-Boc-piperazine, IPA, reflux, 51%; (d) $N_2H_4.H_2O$, EtOH, reflux, 81%; (e) 1,1′-carbonyldiimidazole, DMF, rt; (f) $NaBH_4$, MeOH, rt, 90%; (g) DMF, rt, 62%; and (h) 4 M HCl in 1,4-dioxane, EtOAc, rt, 91%.

https://dx.doi.org/10.1021/acs.jmedchem.0c00002
J. Med. Chem. XXXX, XXX, XXX−XXX

Scheme 6. Synthesis of Amino Alcohol Derivatives of Pimavanserin (Compounds 35a-b)[a]

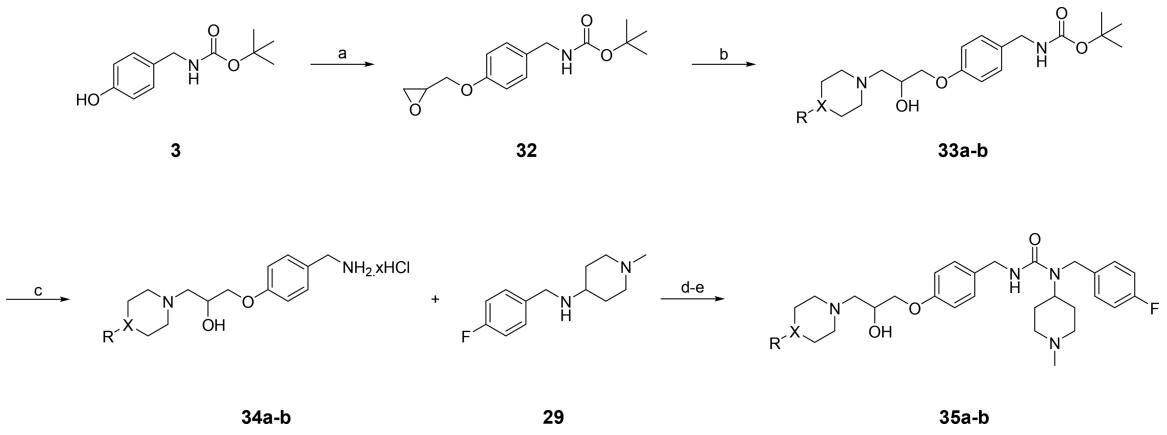

[a]Reagents and conditions: (a) epichlorohydrin, K_2CO_3, ACN, reflux, 37%; (b) 3-(1-piperazinyl)-1,2-benzisothiazole or 6-fluoro-3-(piperidin-4-yl)benzo[d]isoxazole hydrochloride, TEA, IPA, reflux, 42−81%; (c) 4M HCl in 1,4-dioxane, EtOAc, rt, 94−97%; (d) 1,1′-carbonyldiimidazole, DMF, rt; and (e) DMF, rt, 11−23%.

Table 2. SAR Data of Pimavanserin Derivatives

	Structure	% inhibition (1 μM)	IC_{50} (nM)
11	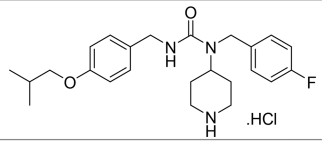	94.25	0.60
12a	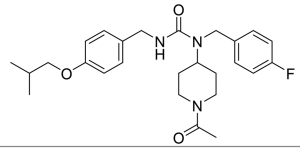	-12.4	nd
12b	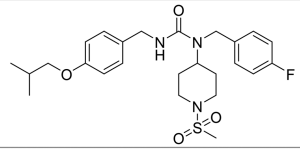	59.03	2018
12c	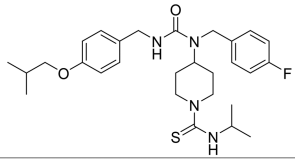	52.37	1126
13	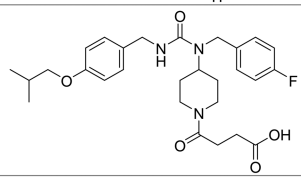	91.47	317.3
1 Pimavanserin	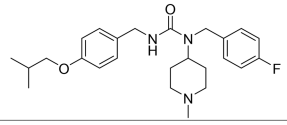	91.61	22

compound **24**. The ring opening reaction of compound **24** with 1-Boc-piperazine yielded compound **25**. Compound **26** was obtained by the phthalimide deprotection of compound **25**, and next it was treated with CDI yielding compound **27**. Under alkaline conditions, compound **27** was coupled with compound **29** (synthesized through the reductive amination of commercially available 4-fluorobenzaldehyde (**7**) and 1-methyl-4-piperidineamine (**28**)) to give compound **30**. Compound **30** underwent acidic deprotection to give compound **31** (Scheme 5). Compound **3** reacted with epichlorohydrin in the presence of a base to afford compound **32**. Compound **32** was coupled with 3-(1-piperazinyl)-1,2-

https://dx.doi.org/10.1021/acs.jmedchem.0c00002
J. Med. Chem. XXXX, XXX, XXX−XXX

Table 3. SAR Data of Amino Acid Derivatives

	Structure	% inhibition (1 μM)	IC_{50} (nM)
14a	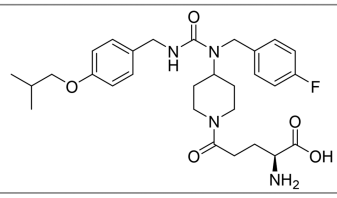	94.1	8.35
15	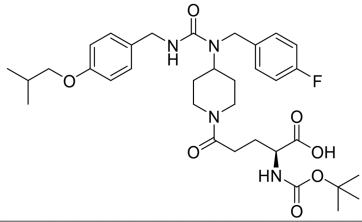	10.47	nd
14b	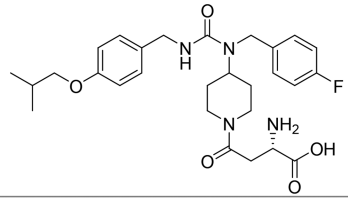	92.61	34.65
14c	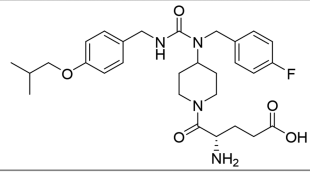	46.51	nd
22	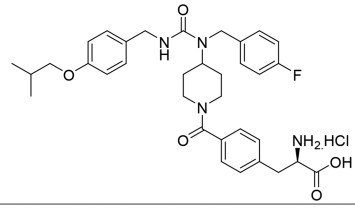	90.69	nd
1 Pimavanserin	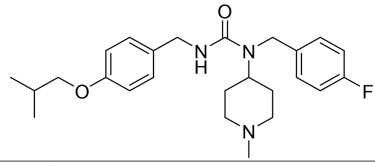	91.61	22

benzisothiazole and 6-fluoro-3-(piperidin-4-yl)benzo[*d*]-isoxazole hydrochloride to yield compounds **33a-b**. Compounds **33a-b** underwent acidic deprotection followed by a reaction with CDI to afford compounds **34a-b**. Compounds **35a-b** were synthesized by the reaction of compounds **34a-b** and compound **29** (Scheme 6).

The synthesized $5HT_{2A}$ antagonists were evaluated for their $5HT_{2A}$ inhibition activities, and the results are summarized in Tables 2−4. In a biological assay at 1 μM concentration, *N*-desmethylpimavanserin (**11**) showed superior in vitro activity compared to pimavanserin; therefore, the nitrogen of desmethylpimavanserin (**11**) was further modified. *N*-acetyl (**12a**), *N*-methylsulfonyl (**12b**), and isopropyl thiourea derivative (**12c**) were evaluated and showed lower activity than pimavanserin. Furthermore, the succinyl derivate of *N*-desmethylpimavanserin was synthesized and evaluated. Succinyl derivative **13** showed submicromolar in vitro potency with an IC_{50} (half maximal inhibitory concentration) value of 317.3 nM. Therefore, carboxylic acid derivatives such as glutamate, aspartate, and tyrosine derivatives were synthesized and evaluated (Table 3). Compound **14a**, a glutamate derivative, improved the potency of pimavanserin with an IC_{50} value of 8.35 nM. Furthermore, *tert*-butoxy carbonyl substitution at the free amine **15** decreased the potency. The aspartate derivative **14b** showed lower potency than **14a**. The reversed glutamate derivative **14c** exhibited a poor inhibition percentage. Next, the tyrosine derivative, **22** was synthesized and was shown to manifest a good in vitro activity; however, it was inferior to that shown by **14a**.

Amino alcohol derivatives obtained from modifications at the isobutoxy position of pimavanserin were synthesized and screened for their ability to inhibit $5HT_{2A}$ (Table 4). The 1-

https://dx.doi.org/10.1021/acs.jmedchem.0c00002
J. Med. Chem. XXXX, XXX, XXX−XXX

Table 4. SAR Data of Amino Alcohol Derivatives

	Structure	% inhibition (1 μM)	IC_{50} (nM)
30	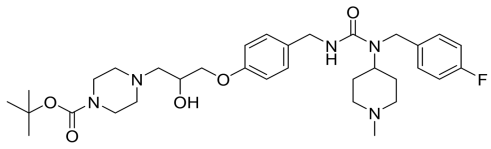	93.62	1.93
31	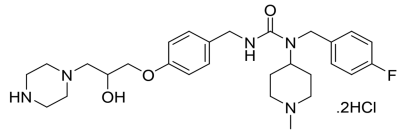	42.41	nd
35a	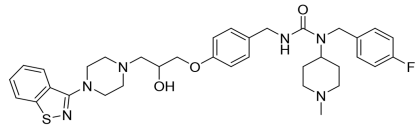	89.82	0.87
35b	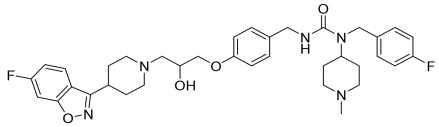	94.6	0.39
1 Pimavanserin	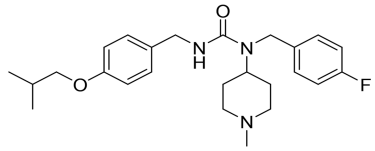	91.61	22

Table 5. PAMPA Results of Compounds 14a and 35b

Compound	Structure	BBB permeability	
		Pe (10^{-6} cm/s)	logPe
14a	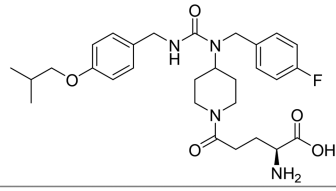	0.00	-10.00
35b	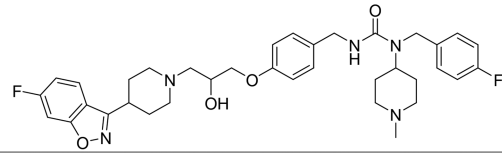	4.79	-5.32

Boc-piperazine derivative **30** exhibited a superior in vitro activity with an IC_{50} value of 1.94 nM. The acidic deprotection of **30** caused a loss of potency in **31**. Next, 3-(1-piperazinyl)-1,2-benzisothiazole and 6-fluoro-3-(piperidin-4-yl)benzo[*d*]-isoxazole derivatives were synthesized and evaluated. Both compounds showed good in vitro potency and **35b** performed better than **35a**, with an IC_{50} value of 0.39 nM.

From the in vitro data, we chose the compounds **14a** and **35b**, with an amino acid and a neutral heterocycle moiety, respectively, for in vitro and in vivo BBB permeability evaluation. The parallel artificial membrane permeation assay

https://dx.doi.org/10.1021/acs.jmedchem.0c00002
J. Med. Chem. XXXX, XXX, XXX−XXX

(PAMPA) was used for BBB permeability prediction, and results are shown in Table 5.

The peripheral residence of compound **14a** was predicted by the low permeability value (10^{-6} cm/s) considering that values under 2.0 predict low permeation. For consistency with the PAMPA results, compound **14a** was evaluated for its BBB penetration by iv injection in rats (Table 6). The brain-to-plasma concentration ratio of compound **14a** was 0.038 after 0.5 h, indicating a limited BBB penetration (Figure 2).

Table 6. Brain/Plasma Ratio in Male ICR Mice (5 mg/kg, IV, Mean ± SD, n = 3) for Compound 14a and 35b

		concentration (ng/mL)		
compound	time (h)	plasma	brain tissue	C_{brain}/C_{plasma}
14a	0.5	415.7 ± 178.0	15.1 ± 5.22	0.038 ± 0.011
35b	0.5	455.3 ± 19.0	740.9 ± 275.5	1.63 ± 0.61

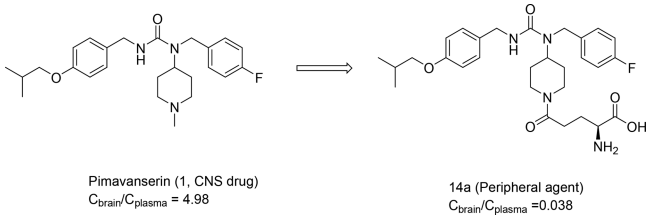

Figure 2. Lead optimization from pimavanserin **1** to compound **14a**.

Furthermore, the unbound fraction of **14a** increased peripheral selectivity (0.02, data not shown). By introducing a glutamic acid moiety, we could drastically increase the peripheral selectivity. Generally, compounds with a brain/plasma ratio greater than 0.3 to 0.5 are considered to have a sufficient CNS diffusion, and compounds with a value of greater than 1 freely cross the BBB, whereas compounds with a brain/plasma ratio smaller than 0.1 may be unable to enter the CNS.[26]

In contrast, compound **35b** seemed to penetrate the BBB at a brain-to-plasma concentration ratio of 1.63 after 0.5 h.

Compound **14a** showed good liver microsomal stability, no significant cytotoxicity in 5 representative mammalian cell lines, and low hERG inhibition (Table 7). For further evaluation, the inhibition percentages of other subtypes of serotonin receptors were screened and compound **14a** showed selective inhibition of $5HT_{2A}$ among the subtypes. In addition, the pharmacokinetic profiles of compound **14a** were studied in rats and are summarized in Table 8. Compound **14** showed reasonable AUC and a half-life of 17 h.

To determine the in vivo efficacy of **14a** for NAFLD, the mice were subjected to a high-fat diet (HFD) for 10 weeks and administered **14a** by daily intraperitoneal injection. Liver tissue weight (Figure 3a) and hepatic triglyceride (TG) accumulation decreased in the mice treated with **14a**, 50 and 100 mg/kg (Figure 3b,c). We also examined the systemic metabolic effects of **14a** considering the $5HT_{2A}$ expression in other metabolic organs such as adipose tissues. Compared to the control, the mice treated with 100 mg/kg **14a** gained less body weight after the HFD and their glucose tolerance was improved (Figure 3d,e). Likewise, body fat decreased while lean body mass increased in mice treated with **14a** (Figure 3f). The mice that received **14a** manifested a fat mass reduction in the inguinal WAT, epididymal WAT, and brown adipose tissue (Figure 3g).

Table 7. Liver Microsomal Stability, Cytotoxicity, and Selectivity Results of Compound 14a

assay	results
liver microsomal phase I stability[a]	rat: 84% remained after 30 min incubation
	human: 89% remained after 30 min incubation
cytotoxicity	VERO IC_{50}: 54.7 μM
	HFL-1 IC_{50}: 55.2 μM
	L929 IC_{50}: 64.0 μM
	NIH 3T3 IC_{50}: 18.2 μM
	CHO-K1 IC_{50}: 51.0 μM
hERG	18.7% inhibition at 10 μM
selectivity[b]	1A: −2.8% inhibition
	1B: 6% inhibition
	2A: 93% inhibition
	2B: 7% inhibition
	2C: 63.8% inhibition
	3: −5% inhibition
	4E: −12.1% inhibition
	6: −18.5% inhibition
	7: 6.3% inhibition

[a]Buspirone was used as a positive control − rat: 15% and human: 4% remained after 30 min of incubation. [b]Test concentration of all assays was 1 μM.

Table 8. Pharmacokinetic Parameters of Compound 14a in Male Rats (iv, 5mpk)

parameters	14a
T1/2 (h)	16.9 ± 11.05
AUC_t (μg·h/mL)	1.91 ± 0.186
AUC_∞ (μg·h/mL)	2.03 ± 0.115
CL (L/h/kg)	2.46 ± 0.137
V_{SS} (L/kg)	11.03 ± 6.62

In addition, they manifested adipocyte size reduction in the inguinal WAT (Figure 3h) and less frequent crownlike structure (CLS) in the epididymal WAT (Figure 3i). Furthermore, BAT was more active in the mice treated with **14a** (Figure 3j). These results demonstrate that **14a** as a selective $5HT_{2A}$ antagonist has therapeutic potential in NAFLD and in the metabolic syndrome.

CONCLUSIONS

A new series of peripheral $5HT_{2A}$ antagonists was synthesized and evaluated for their inhibitory ability. Among them, compound **14a** exhibited a good in vitro activity with an IC_{50} value of 8.35 nM. It also showed liver microsomal stability and no significant inhibition of CYP and hERG. In addition, compound **14a** selectively inhibited $5HT_{2A}$ among other 5HT receptor subtypes. From the in vitro and in vivo BBB permeability study, **14a** proved to be a peripherally acting agent. Compound **14a** improved glucose tolerance in HFD-fed mice. By $5HT_{2A}$ inhibition, it also decreased the liver weight and alleviated lipid accumulation and hepatic steatosis. The treated mice additionally showed decreased fat mass. In conclusion, these newly synthesized peripherally acting $5HT_{2A}$ antagonists have the potential for further development as drugs in the treatment of fatty liver disease.

EXPERIMENTAL SECTION

General. All solvents and chemicals were used as purchased without further purification. All the reported yields are isolated yields

https://dx.doi.org/10.1021/acs.jmedchem.0c00002
J. Med. Chem. XXXX, XXX, XXX−XXX

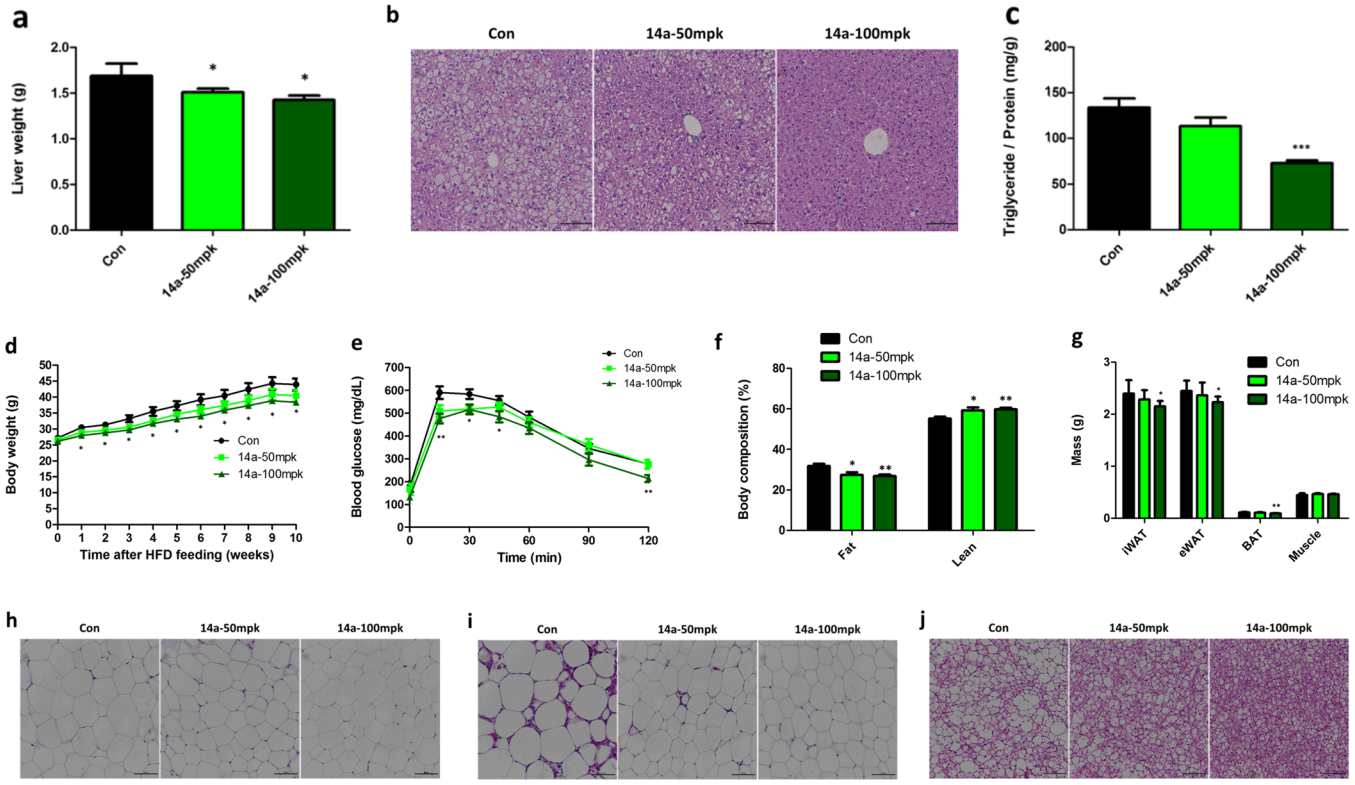

Figure 3. In vivo efficacy of **14a** for HFD-induced NAFLD mice. C57BL/6J mice (12 weeks old) underwent 10 weeks of HFD feeding and for the same period intraperitoneal injections of **14a**. (a) Whole liver weight of HFD-fed control and **14a**-treated mice. (b) Representative liver histology by hematoxylin and eosin staining from HFD-subjected control and **14a**-treated mice. Scale bars, 100 μm. (c) Hepatic triglyceride measurement. (d) Bodyweight trends. (e) Intraperitoneal glucose tolerance test (IPGTT) after 16 h of fasting. (f) Body composition, analyzed by NMR. (g) Inguinal WAT (iWAT), epididymal WAT (eWAT), BAT, and muscle (quadriceps) tissue mass. (h) Representative H&E staining images of (h) iWAT, (i) eWAT, and (j) BAT. The data are presented as mean ± SEM (n = 7 per group). *p < 0.05; **p < 0.01; ***p < 0.00; Con, Control; **14a**-50mpk, **14a** at 50 mg/kg; **14a**-100mpk, **14a** at 100 mg/kg.

after column chromatography or crystallization. ^{1}H NMR spectra and ^{13}C spectra were recorded on a JEOL JNM-ECS400 spectrometer at 400 MHz for ^{1}H NMR and 100 MHz for ^{13}C NMR, respectively. The chemical shift (δ) is expressed in ppm relative to tetramethylsilane (TMS) as an internal standard, and $CDCl_3$, DMSO-d_6, and CD_3OD were used as solvents. Multiplicity of peaks is expressed as s (singlet), d (doublet), t (triplet), q (quartet), dd (doublet of doublets), td (triplet of doublets), qd (quartet of doublets), dt (doublet of triplets), and m (multiplet). HRMS data were obtained by a JMS 700 (JEOL, Japan). Melting points were determined on a Melting Point M-560, purchased from Buchi. Optical rotations were measured on a P-2000 polarimeter, purchased from Jasco. High-performance liquid chromatography (HPLC) analyses were performed with a Waters Agilent HPLC system equipped with a PDA detector and an Agilent SB-C18 column (1.8 μm, 2.1 × 50 mm). The mobile phase consisted of buffer A (ultrapure H_2O containing 0.1% trifluoroacetic acid) and buffer B (chromatographic grade CH_3CN) for method A and buffer C (chromatographic grade MeOH) for method B was applied at a flow rate of 0.3 mL/min.

1-(4-Fluorobenzyl)-3-(4-isobutoxybenzyl)-1-(piperidin-4-yl)urea Hydrochloride (11). Step 1. A mixture of 4-hydroxybenzylamine (**2**) (2 g, 16.239 mmol), di-*tert*-butylcarbonate (7.085 g, 32.478 mmol), and $NaHCO_3$ (3.411 g, 40.598 mmol) in water (30 mL) and methanol (30 mL) were stirred for 18 h at ambient temperature. The reaction mixture was concentrated in vacuo and extracted with ethyl acetate. The combined organic layer was dried over anhydrous Na_2SO_4 and evaporated. The residue was purified by silica gel chromatography to give *tert*-butyl (4-isobutoxybenzyl)carbamate (**3**) (3.45 g, 95%) as a white solid. ^{1}H NMR (400 MHz, chloroform-*d*) δ 7.12 (d, J = 7.6 Hz, 2H), 6.79–6.75 (m, 2H), 5.63 (s, 1H), 4.82 (s, 1H), 4.23 (d, J = 5.2 Hz, 2H), 1.46 (s, 9H).

Step 2. To a solution of compound **3** (3.45 g, 15.452 mmol) in dimethylformamide (12 mL), 1-bromo-2-methylpropane (2.016 mL, 18.543 mmol) and K_2CO_3 (3.203 g, 23.984 mmol) were added and stirred at 80 °C for 16 h. The mixture was cooled to room temperature and extracted with ethyl acetate and water. The combined organic layer was washed with brine and dried over anhydrous Na_2SO_4, filtered, and concentrated. The residue was then purified by silica gel chromatography to provide *tert*-butyl (4-hydroxybenzyl)carbamate (**4**) (1.44 g, 33%) as a white solid. ^{1}H NMR (400 MHz, DMSO-d_6) δ 7.29 (t, J = 6.0 Hz, 1H), 7.13 (d, J = 8.5 Hz, 2H), 6.85 (d, J = 8.5 Hz, 2H), 4.03 (d, J = 6.1 Hz, 2H), 3.70 (d, J = 6.4 Hz, 2H), 2.04–1.94 (m, 1H), 1.38 (s, 9H), 0.96 (d, J = 6.7 Hz, 6H).

Step 3. Compound **4** (1.44 g, 5.154 mmol) in ethyl acetate (6 mL) was treated with 4 M solution of hydrogen chloride in 1,4-dioxane (6 mL). The reaction mixture was stirred for 4 h at ambient temperature. The mixture was distilled and the product was collected by filtration and washed with ethyl acetate to yield (4-isobutoxyphenyl)-methanamine hydrochloride (**5**) (1.025 g, 92%) as a white solid. ^{1}H NMR (400 MHz, DMSO-d_6) δ 8.35 (s, 2H), 7.39 (d, J = 8.2 Hz, 2H), 6.95 (d, J = 8.5 Hz, 2H), 3.92 (s, 2H), 3.74 (d, J = 6.7 Hz, 2H), 2.05–1.95 (m, 1H), 0.97 (d, J = 6.7 Hz, 6H).

Step 4. A mixture of compound **5** (1.025 g, 4.752 mmol) and 1,1′-carbonyldiimidazole (847.51 mg, 5.227 mmol) in dimethylformamide (4 mL) was stirred for 16 h at ambient temperature. The mixture was extracted with ethyl acetate and water. The combined organic layer was washed with brine and dried over anhydrous Na_2SO_4, filtered, and evaporated. The residue was purified by silica gel chromatography to give *N*-(4-isobutoxybenzyl)-1*H*-imidazole-1-carboxamide (**6**) (1.38 g, 68%) as a pale yellow oil. ^{1}H NMR (400 MHz, chloroform-*d*) δ 8.50 (t, J = 4.7 Hz, 1H), 8.09 (s, 1H), 7.48 (s, 1H), 7.17 (d, J = 8.5 Hz,

https://dx.doi.org/10.1021/acs.jmedchem.0c00002
J. Med. Chem. XXXX, XXX, XXX−XXX

2H), 6.82−6.80 (m, 3H), 4.42 (d, J = 5.5 Hz, 2H), 3.67 (d, J = 6.4 Hz, 2H), 2.10−2.00 (m, 1H), 1.00 (d, J = 6.7 Hz, 6H).

Step 5. 4-Fluorobenzaldehyde (**7**) (1.702 mL, 16.115 mmol) and 4-amino-1-bocpiperidine (**8**) (3.227 g, 16.115 mmol) in methanol (30 mL) were stirred for 16 h at ambient temperature. $NaBH_4$ (1.837 g, 48.344 mmol) was added to the reaction mixture in portions, and the resulting mixture was stirred for 16 h. The mixture was evaporated and extracted with ethyl acetate and water. The combined organic layer was dried over anhydrous Na_2SO_4, filtered, and concentrated. The residue was then purified by silica gel chromatography to give *tert*-butyl 4-((4-fluorobenzyl)amino)piperidine-1-carboxylate (**9**) (3.24 g, 65%) as a white solid. ^{1}H NMR (400 MHz, chloroform-d) δ 7.32−7.27 (m, 2H), 7.03−6.98 (m, 2H), 4.03 (s, 2H), 3.79 (s, 2H), 2.80 (t, J = 11.6 Hz, 2H), 2.68−2.61 (m, 1H), 1.85 (d, J = 11.3 Hz, 2H), 1.45 (s, 9H), 1.34−1.24 (m, 2H).

Step 6. A mixture of compound **6** (1.38 g, 5.049 mmol), compound **9** (1.557 g, 5.049 mmol), and K_2CO_3 (1.047 g, 7.573 mmol) in dimethylformamide (6 mL) were stirred for 18 h at ambient temperature. The reaction mixture was extracted with ethyl acetate and water. The combined organic layer was dried over anhydrous Na_2SO_4, filtered, and evaporated. The residue was then purified by silica gel chromatography to give *tert*-butyl 4-(1-(4-fluorobenzyl)-3-(4-isobutoxybenzyl)ureido)piperidine-1-carboxylate (**10**) (1.930 g, 74%) as a colorless oil. ^{1}H NMR (400 MHz, DMSO-d_6) δ 7.23 (dd, J = 8.6, 5.4 Hz, 2H), 7.17−7.06 (m, 4H), 6.89 (t, J = 5.6 Hz, 1H), 6.91−6.81 (m, 2H), 4.40 (s, 2H), 4.18 (d, J = 5.5 Hz, 2H), 4.14−3.99 (m, 1H), 3.94−3.91(m, 2H), 3.74−3.67 (m, 2H), 2.68 (s, 2H), 2.03−1.93 (m, 1H), 1.50−1.30 (m, 4H), 1.36 (s, 9H), 0.96 (dd, J = 6.6, 1.7 Hz, 6H).

Step 7. A 4 M hydrogen chloride solution in 1,4-dioxane (6 mL) was added to the solution of compound **10** (1.930 g, 3.757 mmol) in ethyl acetate (6 mL). The resulting mixture was stirred for 6 h at ambient temperature. The mixture was concentrated in vacuo and the product was collected by filtration (1.5 g, 88%) as a white solid. ^{1}H NMR (400 MHz, methanol-d_4) δ 7.30−7.22 (m, 2H), 7.14−7.01 (m, 4H), 6.84−6.78 (m, 2H), 4.50 (s, 2H), 4.37−4.24 (m, 3H), 3.71 (d, J = 6.5 Hz, 2H), 3.66 (s, 1H), 3.45−3.37 (m, 2H), 3.04 (td, J = 12.7, 4.4 Hz, 2H), 2.09−2.00 (m, 1H), 1.95−1.87 (m, 4H), 1.02 (d, J = 6.7 Hz, 6H); ^{13}C NMR (100 MHz, DMSO-d_6) δ 162.19, 159.78, 157.49, 157.33, 136.61, 132.92, 128.38, 128.30, 128.26, 115.02, 114.81, 114.08, 73.75, 66.39, 50.14, 44.24, 43.11, 42.99, 27.74, 26.63, 19.09; mp 171−173 °C; HRMS (FAB) m/z calculated for $C_{24}H_{33}FN_3O_2$ $[M + H]^+$ 414.2557, found 414.2557; HPLC purity 95.9277% (method A).

(*S*)-2-Amino-5-(4-(1-(4-fluorobenzyl)-3-(4-isobutoxybenzyl)-ureido)piperidin-1-yl)-5-oxopentanoic Acid (14a). Step 1. A mixture of compound **11** (250 mg, 0.557 mmol), 1-benzyl *N*-carbobenzoxy-L-glutamate (207 mg, 0.557 mmol), EDCI (267.12 mg, 1.393 mmol), HOBt (113.04 mg, 0.836 mmol), and DIPEA (0.341 mL, 1.951 mmol) in dimethylforamide (2 mL) was stirred for 16 h at ambient temperature. The reaction mixture was extracted with ethyl acetate and water. The combined organic layer was dried over anhydrous Na_2SO_4, filtered, and evaporated. The residue was then purified by silica gel column chromatography go give benzyl (*S*)-2-(((benzyloxy)carbonyl)amino)-5-(4-(1-(4-fluorobenzyl)-3-(4-isobutoxybenzyl)ureido)piperidin-1-yl)-5-oxopentanoate (260 mg, 61%) as a colorless oil.

Step 2. To a solution of benzyl (*S*)-2-(((benzyloxy)carbonyl)-amino)-5-(4-(1-(4-fluorobenzyl)-3-(4-isobutoxybenzyl)ureido)-piperidin-1-yl)-5-oxopentanoate in methanol (100 mL), Pd/C (100 mg) was added and stirred for 2 h under a hydrogen atmosphere. The reaction mixture was filtered through Celite and evaporated. The residue was filtered with diethyl ether to give compound **14a** (138 mg, 75%) as a pale gray solid. ^{1}H NMR (400 MHz, methanol-d_4) δ 7.27−7.18 (m, 2H), 7.12−7.06 (m, 2H), 7.06−6.96 (m, 2H), 6.84−6.76 (m, 2H), 4.58 (d, J = 13.7 Hz, 1H), 4.47 (s, 2H), 4.35−4.27 (d, J = 4.5 Hz, 3H), 4.01−3.92 (m, 1H), 3.71 (d, J = 6.5 Hz, 2H), 3.58 (dt, J = 7.7, 5.8 Hz, 1H), 3.17−3.06 (m, 1H), 2.69−2.54 (m, 3H), 2.14−1.96 (m, 3H), 1.77−1.45 (m, 4H), 1.02 (d, J = 6.7 Hz, 6H); ^{13}C NMR (100 MHz, DMSO-d_6) δ 170.31, 170.00, 162.09, 159.69, 157.47, 136.91, 133.05, 128.35, 128.27, 128.18, 114.88, 114.67, 114.09, 73.77, 53.70, 52.74, 44.40, 44.05, 43.12, 40.73, 30.53, 29.96, 29.00, 27.74, 26.77, 19.10; mp 147−149 °C; HRMS (FAB) m/z calculated for $C_{29}H_{40}FN_4O_5$ $[M + H]^+$ 543.2983, found 543.2984; HPLC purity 98.2157% (method A); $[\alpha]_D$: −0.1586 (c 1.0406, methanol).

In Vitro Activity. The pimavanserin derivatives were evaluated at a concentration of 1 μM for their antagonist activity on the 5-HT_{2A} receptor.[27,28] 5-HT2A stable HEK293 cells were seeded in a 96-well plate (Costar; 3603) at a density of 8 ∼ 9 × 10^4 in 100 μL of minimum essential medium (Welgene; LM007-86) containing 10% dialyzed fetal bovine serum (Gibco; 30067-334) and 1% penicillin/streptomycin (Gibco; 15140-122) and kept in a 37 °C incubator for 24 h. The cells were stained with 100 μL of cytosolic calcium dye using the FLIPR calcium 6 assay solution (Molecular devices, #R8190) supplemented with 2.5 mM probenecid (Sigma; P8761) and incubated for 1 h at 37 °C. After 1 h, the designated amount of the compound was treated in each well and incubated for another 1 h at 37 °C. Then, the cells were loaded in a Flexstation 3 microplate reader (Molecular Devices; FlexStaion) and 50 μL of 5 μM 5-HT2A (serotonin hydrochloride, Sigma; H9523) was injected from a source plate (Nunc 96-well polystyrene conical bottom MicroWell Plate, Thermo; 249662) and the florescence intensity (Ex/Em-485nm/525nm) was measured.

Blood−Brain Barrier (BBB) Penetration Study in Mice. The previously reported methods were used for the BBB penetration of **14a** in mice.[29] Male ICR mice were intravenously administered **14a** (5 mg/kg) prepared as a solution (DMSO: PEG400: saline = 5:40:55, v/v/v %). After 0.5 h, the mice were euthanized using CO_2 gas, and the blood was collected from the heart immediately and the plasma was separated by centrifugation at 3000 rpm for 10 min at 4 °C. The rest of the blood was washed out from the circulation by performing cardiac perfusion with physiological saline containing 10 U/mL heparin. Then, the brain was removed from the skull and added to three volumes of PBS buffer per weight, homogenized, and stored at −20 °C until analyzed by LC-MS/MS. The concentrations of **14a** in plasma and brain samples were determined using an API 4000 Q trap mass spectrometer (Applied Biosystems, Foster City, CA, USA) coupled with a 1200 series HPLC system (Agilent, Santa Clara, CA, USA). Isocratic elution was used with 80% acetonitrile and 20% water with 0.1% formic acid for the separation of analytes. The total run time was 3 min, and the flow rate was 0.3 mL/min.

Pharmacokinetic Study in Rats. The compound was administered by intravenous injection (5 mg/kg) in male SD rats. It was prepared with the same vehicle as was used in the BBB penetration study. Blood samples were collected at time points of 0.083, 0.167, 0.5, 1, 2, 4, 8, and 24 h post-injection. After the separation of plasma by centrifugation, the concentration of **14a** in plasma was determined by the LC−MS/MS system. Pharmacokinetic parameters were obtained by noncompartmental analysis using the WinNolin program (ver. 6.3, Pharsight, Mountain View, CA).

In Vivo Efficacy for NAFLD. C57BL/6J mice were purchased from the Charles River Japan (Yokohama, Japan). The mice were housed in climate-controlled, specific pathogen-free barrier facilities under a 12 h light−dark cycle, and chow and water were provided ad libitum. Mice (12 weeks old) were fed with a HFD (Research Diet D12492, 60% fat calories) for 10 weeks and administered **14a** by daily intraperitoneal injection for the same period. On the ninth week of HFD feeding, intraperitoneal glucose tolerance test (2 g/kg of glucose) was performed and body composition was measured by NMR analysis (LF50 BCA-analyzer, Bruker) a day before sacrifice. All animal experiments complied with the relevant ethical regulations. Experimental protocols for this study were approved by the institutional animal care and use committee at the Korea Advanced Institute of Science and Technology.

Quantification of Hepatic Triglyceride. Liver tissues were homogenized in 5% NP-40 using FastPrep-24 (MP Biomedicals). To solubilize fat, the homogenates were heated to 95 °C for 5 min and cooled at 23 °C and repeated. A triglyceride reagent (Sigma-Aldrich) or PBS was added and incubated at 37 °C for 30 min to hydrolyze TG

https://dx.doi.org/10.1021/acs.jmedchem.0c00002
J. Med. Chem. XXXX, XXX, XXX−XXX

into glycerol. For the colorimetric assay of hydrolyzed TG levels, samples were incubated with a free glycerol reagent (Sigma-Aldrich) at 37 °C for 5 min. Differences in absorbance at 540 nm between hydrolyzed or nonhydrolyzed TG were quantified using a glycerol standard (Sigma-Aldrich). TG contents were normalized by the protein concentrations of homogenates, which were measured with a BCA protein assay kit (Thermo Scientific).

Histological Analysis. Mouse liver, inguinal white adipose tissue, epididymal white adipose tissue, and interscapular brown adipose tissue were harvested and fixed in 10% neutral buffered formalin solution (Sigma-Aldrich) and embedded in paraffin. The 5 μm-thick tissue sections were deparaffinized, rehydrated, and stained with hematoxylin and eosin (H&E).

■ ASSOCIATED CONTENT

Supporting Information

The Supporting Information is available free of charge at https://pubs.acs.org/doi/10.1021/acs.jmedchem.0c00002.

Synthesis procedures, ^{1}H NMR, ^{13}C NMR, HRMS spectra, and HPLC assessment of purity for all the final compounds, dose response curve, and selectivity data of compound **14a** (PDF)

Molecular formula strings (CSV)

■ AUTHOR INFORMATION

Corresponding Authors

Hail Kim − *Graduate School of Medical Science and Engineering, Korea Advanced Institute of Science and Technology, Daejeon 34141, Republic of Korea*; Phone: +82-42-350-4243; Email: hailkim@kaist.edu; Fax: +82-42-350-4287

Jin Hee Ahn − *Department of Chemistry, Gwangju Institute of Science and Technology, Gwangju 61005, Republic of Korea; R&D center, JD Bioscience, Gwangju 61005, Republic of Korea*; orcid.org/0000-0002-6957-6062; Phone: +82-62-715-4621; Email: jhahn@gist.ac.kr

Authors

Minhee Kim − *Department of Chemistry, Gwangju Institute of Science and Technology, Gwangju 61005, Republic of Korea*; orcid.org/0000-0001-5384-7342

Inseon Hwang − *Graduate School of Medical Science and Engineering, Korea Advanced Institute of Science and Technology, Daejeon 34141, Republic of Korea*

Haushabhau S. Pagire − *Department of Chemistry, Gwangju Institute of Science and Technology, Gwangju 61005, Republic of Korea*

Suvarna H. Pagire − *Department of Chemistry, Gwangju Institute of Science and Technology, Gwangju 61005, Republic of Korea*

Wonsuk Choi − *Graduate School of Medical Science and Engineering, Korea Advanced Institute of Science and Technology, Daejeon 34141, Republic of Korea*

Won Gun Choi − *Graduate School of Medical Science and Engineering, Korea Advanced Institute of Science and Technology, Daejeon 34141, Republic of Korea*

Jihyeon Yoon − *Department of Chemistry, Gwangju Institute of Science and Technology, Gwangju 61005, Republic of Korea*

Won Mi Lee − *Department of Chemistry, Gwangju Institute of Science and Technology, Gwangju 61005, Republic of Korea*

Jin Sook Song − *Bio & Drug Discovery Division, Korea Research Institute of Chemical Technology, Daejeon, Republic of Korea*

Eun Kyung Yoo − *Leading-edge Research Center for Drug Discovery and Development for Diabetes and Metabolic Disease, Kyungpook National University Hospital, Daegu 41010, Republic of Korea*

Seung Mi Lee − *Leading-edge Research Center for Drug Discovery and Development for Diabetes and Metabolic Disease, Kyungpook National University Hospital, Daegu 41010, Republic of Korea*

Mi-jin Kim − *Leading-edge Research Center for Drug Discovery and Development for Diabetes and Metabolic Disease, Kyungpook National University Hospital, Daegu 41010, Republic of Korea*

Myung Ae Bae − *Bio & Drug Discovery Division, Korea Research Institute of Chemical Technology, Daejeon, Republic of Korea*

Dooseop Kim − *R&D center, JD Bioscience, Gwangju 61005, Republic of Korea*

Heejong Lee − *R&D center, JD Bioscience, Gwangju 61005, Republic of Korea*

Eun-Young Lee − *R&D center, JD Bioscience, Gwangju 61005, Republic of Korea*

Jae-Han Jeon − *Department of Internal Medicine, School of Medicine, Kyungpook National University, Kyungpook National University Hospital, Daegu 41944, Republic of Korea; Leading-edge Research Center for Drug Discovery and Development for Diabetes and Metabolic Disease, Kyungpook National University Hospital, Daegu 41010, Republic of Korea*

In-Kyu Lee − *Department of Internal Medicine, School of Medicine, Kyungpook National University, Kyungpook National University Hospital, Daegu 41944, Republic of Korea; Leading-edge Research Center for Drug Discovery and Development for Diabetes and Metabolic Disease, Kyungpook National University Hospital, Daegu 41010, Republic of Korea*

Complete contact information is available at: https://pubs.acs.org/10.1021/acs.jmedchem.0c00002

Author Contributions

‡M.K. and I.H. equally contributed to this work.

Notes

The authors declare no competing financial interest.

■ ACKNOWLEDGMENTS

This work was supported by grants from the Korea Health Industry Development Institute (KHIDI), funded by the Ministry of Health and Welfare (HI16C1501, HI12C1006), the Ministry of Science, ICT and Future Planning(MSIP)/National Research Foundation of Korea(NRF) (2016M3A9B6902868).

■ ABBREVIATIONS

NAFLD, nonalcoholic fatty liver disease; NASH, nonalcoholic steatohepatitis; TPH, tryptophan hydroxylase; DKO, double knockout; WAT, white adipose tissue; BAT, brown adipose tissue; NAS, NAFLD activity score; TG, hepatic triglyceride; CDI, 1,1′-carbonyldiimidazole; MeOH, methanol; EtOAc, ethyl acetate; DIPEA, *N*,*N*-diisopropylethylamine; EDCI, 1-ethyl-3-(3-diemthylaminopropyl)carbodiimide; HOBt, hydroxybenzotriazole; EtOH, ethanol; TEA, triethylamine; dppf, 1,1′-bis(dipheynlphosphino)ferrocene; ACN, acetonitrile; IPA, isopropylalcohol; HFD, high-fat diet; CLS, crownlike structure; IPGTT, intraperitoneal glucose tolerance test

https://dx.doi.org/10.1021/acs.jmedchem.0c00002
J. Med. Chem. XXXX, XXX, XXX−XXX

REFERENCES

(1) Younossi, Z.; Anstee, Q. M.; Marietti, M.; Hardy, T.; Henry, L.; Eslam, M.; George, J.; Bugianesi, E. Global burden of NAFLD and NASH: Trends, Predictions, Risk Factors and Prevention. *Nat. Rev. Gastroenterol. Hepatol.* **2018**, *15*, 11−20.

(2) Musso, G.; Gambino, R.; Cassader, M. Recent Insights into Hepatic Lipid Metabolism in Non-alcoholic Fatty Liver Disease (NAFLD). *Prog. Lipid Res.* **2009**, *48*, 1−26.

(3) Pais, R.; Barritt, A. S., 4th; Calmus, Y.; Scatton, O.; Runge, T.; Lebray, P.; Poynard, T.; Ratziu, V.; Conti, F. NAFLD and Liver Transplantation: Current Burden and Expected Challenges. *J. Hepatol.* **2016**, *65*, 1245−1257.

(4) Michelotti, G. A.; Machado, M. V.; Diehl, A. M. NAFLD, NASH and Liver Cancer. *Nat. Rev. Gastroenterol. Hepatol.* **2013**, *10*, 656.

(5) Kim, D.-Y.; Camilleri, M. Serotonin: A Mediator of the Brain−Gut Connection. *Am. J. Gastroenterol.* **2000**, *95*, 2698.

(6) Walther, D. J.; Peter, J.-U.; Bashammakh, S.; Hörtnagl, H.; Voits, M.; Fink, H.; Bader, M. Synthesis of Serotonin by a Second Tryptophan Hydroxylase Isoform. *Science* **2003**, *299*, 76.

(7) Keszthelyi, D.; Troost, F. J.; Masclee, A. A. M. Understanding the Role of Tryptophan and Serotonin Metabolism in Gastrointestinal Function. *Neurogastroenterol. Motil.* **2009**, *21*, 1239−1249.

(8) Zhang, X.; Beaulieu, J.-M.; Sotnikova, T. D.; Gainetdinov, R. R.; Caron, M. G. Tryptophan Hydroxylase-2 Controls Brain Serotonin Synthesis. *Science* **2004**, *305*, 217.

(9) Berger, M.; Gray, J. A.; Roth, B. L. The Expanded Biology of Serotonin. *Annu. Rev. Med.* **2009**, *60*, 355−366.

(10) Donaldson, Z. R.; Nautiyal, K. M.; Ahmari, S. E.; Hen, R. Genetic Approaches for Understanding the Role of Serotonin Receptors in Mood and Behavior. *Curr. Opin. Neurobiol.* **2013**, *23*, 399−406.

(11) Crockett, M. J.; Clark, L.; Tabibnia, G.; Lieberman, M. D.; Robbins, T. W. Serotonin Modulates Behavioral Reactions to Unfairness. *Science* **2008**, *320*, 1739.

(12) Roth, B. L.; Hanizavareh, S. M.; Blum, A. E. Serotonin Receptors Represent Highly Favorable Molecular Targets for Cognitive Enhancement in Schizophrenia and Other Disorders. *Psychopharmacology* **2004**, *174*, 17−24.

(13) Portas, C. M.; Bjorvatn, B.; Ursin, R. Serotonin and the Sleep/wake Cycle: Special Emphasis on Microdialysis Studies. *Prog. Neurobiol.* **2000**, *60*, 13−35.

(14) D'Agostino, G.; Lyons, D.; Cristiano, C.; Lettieri, M.; Olarte-Sanchez, C.; Burke, L. K.; Greenwald-Yarnell, M.; Cansell, C.; Doslikova, B.; Georgescu, T.; Martinez de Morentin, P. B.; Myers, M. G., Jr.; Rochford, J. J.; Heisler, L. K. Nucleus of the Solitary Tract Serotonin 5-HT2C Receptors Modulate Food Intake. *Cell Metab.* **2018**, *28*, 619−630.e5.

(15) Oh, C.-M.; Park, S.; Kim, H. Serotonin as a New Therapeutic Target for Diabetes Mellitus and Obesity. *Diabetes Metab. J.* **2016**, *40*, 89−98.

(16) Oh, C.-M.; Namkung, J.; Go, Y.; Shong, K. E.; Kim, K.; Kim, H.; Park, B.-Y.; Lee, H. W.; Jeon, Y. H.; Song, J.; Shong, M.; Yadav, V. K.; Karsenty, G.; Kajimura, S.; Lee, I.-K.; Park, S.; Kim, H. Regulation of Systemic Energy Homeostasis by Serotonin in Adipose Tissues. *Nat. Commun.* **2015**, *6*, 6794.

(17) Watanabe, H.; Akasaka, D.; Ogasawara, H.; Sato, K.; Miyake, M.; Saito, K.; Takahashi, Y.; Kanaya, T.; Takakura, I.; Hondo, T.; Chao, G.; Rose, M. T.; Ohwada, S.; Watanabe, K.; Yamaguchi, T.; Aso, H. Peripheral Serotonin Enhances Lipid Metabolism by Accelerating Bile Acid Turnover. *Endocrinology* **2010**, *151*, 4776−4786.

(18) Savelieva, K. V.; Zhao, S.; Pogorelov, V. M.; Rajan, I.; Yang, Q.; Cullinan, E.; Lanthorn, T. H. Genetic Disruption of Both Tryptophan Hydroxylase Genes Dramatically Reduces Serotonin and Affects Behavior in Models Sensitive to Antidepressants. *PLoS One* **2008**, *3*, No. e3301.

(19) Zhang, X.; Wang, X.; Yin, H.; Zhang, L.; Feng, A.; Zhang, Q.-X.; Lin, Y.; Bao, B.; Hernandez, L. L.; Shi, G.-P.; Liu, J. Functional Inactivation of Mast Cells Enhances Subcutaneous Adipose Tissue Browning in Mice. *Cell Rep.* **2019**, *28*, 792−803.e4.

(20) Yabut, J. M.; Desjardins, E. M.; Chan, E. J.; Day, E. A.; Leroux, J. M.; Wang, B.; Crane, E. D.; Wong, W.; Morrison, K. M.; Crane, J. D.; Khan, W. I.; Steinberg, G. R. Genetic Deletion of Mast Cell Serotonin Synthesis Prevents the Development of Obesity and Insulin Resistance. *Nat. Commun.* **2020**, *11*, 463.

(21) Crane, J. D.; Palanivel, R.; Mottillo, E. P.; Bujak, A. L.; Wang, H.; Ford, R. J.; Collins, A.; Blümer, R. M.; Fullerton, M. D.; Yabut, J. M.; Kim, J. J.; Ghia, J.-E.; Hamza, S. M.; Morrison, K. M.; Schertzer, J. D.; Dyck, J. R. B.; Khan, W. I.; Steinberg, G. R. Inhibiting Peripheral Serotonin Synthesis Reduces Obesity and Metabolic Dysfunction by Promoting Brown Adipose Tissue Thermogenesis. *Nat. Med.* **2015**, *21*, 166.

(22) Namkung, J.; Shong, K. E.; Kim, H.; Oh, C.-M.; Park, S.; Kim, H. Inhibition of Serotonin Synthesis Induces Negative Hepatic Lipid Balance. *Diabetes Metab. J.* **2018**, *42*, 233−243.

(23) Choi, W.; Namkung, J.; Hwang, I.; Kim, H.; Lim, A.; Park, H. J.; Lee, H. W.; Han, K.-H.; Park, S.; Jeong, J.-S.; Bang, G.; Kim, Y. H.; Yadav, V. K.; Karsenty, G.; Ju, Y. S.; Choi, C.; Suh, J. M.; Park, J. Y.; Park, S.; Kim, H. Serotonin Signals through a Gut-liver Axis to Regulate Hepatic Steatosis. *Nat. Commun.* **2018**, *9*, 4824.

(24) Osawa, Y.; Kanamori, H.; Seki, E.; Hoshi, M.; Ohtaki, H.; Yasuda, Y.; Ito, H.; Suetsugu, A.; Nagaki, M.; Moriwaki, H.; Saito, K.; Seishima, M. L-Tryptophan-mediated Enhancement of Susceptibility to Nonalcoholic Fatty Liver Disease Is Dependent on the Mammalian Target of Rapamycin. *J. Biol. Chem.* **2011**, *286*, 34800−34808.

(25) Markham, A. Pimavanserin: First Global Approval. *Drugs* **2016**, *76*, 1053−1057.

(26) Reichel, A. The Role of Blood-Brain Barrier Studies in the Pharmaceutical Industry. *Curr. Drug Metab.* **2006**, *7*, 183−203.

(27) Seitz, P. K.; Bremer, N. M.; McGinnis, A. G.; Cunningham, K. A.; Watson, C. S. Quantitative Changes in Intracellular Calcium and Extracellular-regulated Kinase Activation Measured in Parallel in CHO Cells Stably Expressing Serotonin (5-HT) 5-HT2A or 5-HT2C receptors. *BMC Neurosci.* **2012**, *13*, 25.

(28) Ding, L.; He, S.; Wu, W.; Jin, H.; Zhu, P.; Zhang, J.; Wang, T.; Yuan, Y.; Yan, X. Discovery and Structure-Based Optimization of 6-Bromotryptamine Derivatives as Potential 5-HT2A Receptor Antagonists. *Molecules* **2015**, *20*, 17675−17683.

(29) Lee, J. H.; Bok, J. H.; Park, S. B.; Pagire, H. S.; Na, Y.-J.; Rim, E.; Jung, W. H.; Song, J. S.; Kang, N. S.; Seo, H. W.; Jung, K.-Y.; Lee, B. H.; Kim, K. Y.; Ahn, J. H. Optimization of Cyclic Sulfamide Derivatives as 11β-hydroxysteroid Dehydrogenase 1 Inhibitors for the Potential Treatment of Ischemic Brain Injury. *Bioorg. Med. Chem. Lett.* **2020**, *30*, 126787.

https://dx.doi.org/10.1021/acs.jmedchem.0c00002
J. Med. Chem. XXXX, XXX, XXX−XXX